TRADEOFFS IN DRIFT CHAMBER DESIGN*

Abraham Seiden
Institute for Particle Physics
University of California
Santa Cruz, California 95064

INTRODUCTION

For the physics of the future, at or above 100 GeV center of mass energy, tracking devices will need: 1) Good segmentation, since particle densities are large. 2) Many samples along each track for pattern recognition, momentum resolution, and possibly dE/dx measurement. As an example, to do a good job separating two high momentum tracks from hadronic decay of the Z^0, angular segmentation ~ 10 mrad is required; typical nearest neighbor tracks of average momentum are separated by ~ 100 mrad.[1] If we multiply 10 mrad by 1 meter we get a track separation of 1 cm. Although small this is still large enough that the solutions to the tracking problem developed over the past 5 years are applicable. Thus the central detectors presented in the LEP Letters of Intent are typically outgrowths of existing devices.

One solution to the tracking problem is to make a chamber with many small cells; cell full-widths ~ 1 to 2 cm would be needed.[2] This requires many wires and electronics channels, however each channel is relatively simple in design.

An alternative design, still of the axial type, is to make a chamber with large cells containing several sense wires per cell.[3] These chambers have many fewer wires than in the case of small cells, however multi-hit electronics is needed. The electronics must not only allow recording of several hits, but also suppress the long 1/t tail of a drift chamber pulse so that later hit information is not degraded by earlier pulses.[4] This type of chamber has the advantage that most of the very good precision of the drift chamber is available at the pattern recognition stage of track finding since the uniform field over most of the drift path makes a simple linear space-time relation quite accurate. For this reason a local solution of the left-right ambiguity is possible if the wires are slightly (~ position resolution) staggered, and an accurate local tangent vector to the track can be found by using the times measured by two nearby wires. For tracks coming from the origin this allows a local calculation of the transverse momentum since the radius of curvature is given by:

$$R = \frac{1}{2}\sqrt{\rho^2 + \left(\frac{d\rho}{d\phi}\right)^2},$$

where ρ and ϕ are the cylindrical coordinates of the track.

A third solution is provided by the TPC[5] and other devices where the sense wires are at the end of the drift volume. These chambers have had, typically, longer drift spaces than the others and have the advantage that no left-right ambiguity exists. I will not discuss these since they are extensively covered in several other contributions.

GENERAL CONSIDERATIONS

Drift chamber performance can be characterized by measurement precision for tracks, ability to separate nearby tracks, ease of pattern recognition, and dE/dx information provided. I will discuss aspects of each of these except for dE/dx which is extensively covered in other conference contributions. The choice of including dE/dx measurement will strongly influence the number of track samples desired, the choice of gas, gas gain, and gas pressure for the chamber.

Momentum Resolution

If we ignore multiple scattering, for large N:

$$\frac{\Delta p_\perp}{p_\perp^2} \sim \frac{\sigma}{BR^2\sqrt{N}},$$

where: σ = spatial resolution, B = magnetic field, R = track length, N = number of measurements. As an example: σ = 200 μm, B = 5 kG, R = 1.5 m, N = 30 gives:

$$\frac{\Delta p_\perp}{p_\perp^2} = .003\ \text{GeV}^{-1},$$

a value which is desirable for physics at the Z^0.

The small cell option, taking 30 equally spaced layers, cell full-width = 1.5 cm, R = 1.5 m, would require 10,000 cells.

Since a large radius R forces the remainder of a detector to be large and expensive, increasing B or decreasing σ would be advantageous since it would allow the same precision for a smaller radius.

Lorentz-Angle. For an axial chamber in a solenoidal field, drift takes place at an angle to the electric field. This angle, $\theta_L \sim \frac{v_{Drift}B}{E} \sim 15^o$ to 20^o for $v_{Drift} \simeq 5$ cm/μsec, B = 4 kG, E = 1 kV/cm. The Lorentz-Angle widens the ionization arrival time spectrum at the sense wire for tracks normally incident on the cell, it makes the cell behavior left-right asymmetric, and also makes it more difficult to associate hits in a multi-wire cell for tracks crossing cell boundaries.

Increasing the Lorentz-Angle substantially beyond 20^o would be detrimental to the chamber performance for an axial drift chamber, especially one with large cells. This means that if one wants a B value >> 4 kG, it would be good to reduce v_{Drift} or increase E accordingly. A gas mixture with small v_{Drift}, saturated velocity, and low diffusion for the drifting electrons would be very useful.[6] An example of the dependence of E on the cell geometry is discussed in a later section.

Diffusion in Gases. For the large drift chambers now functioning, the expected contribution to the resolution from the diffusion of ionization electrons is much smaller than the 200 μm resolution gotten in practice. This implies that improvement in resolution could be gotten if various systematic factors such as wire alignment and sag, as well as an understanding of the time to space relation were better controlled. Figure 1 shows a model calculation of the resolution expected versus impact parameter for several gas choices, based on diffusion and ionization statistics.[7] We see that if we are satisfied with 200 μm resolution, fairly large cells (~ 5 cm half-width) could be used for a 1 atmosphere 50/50 Ar/Ethane mix before substantial contributions from diffusion occur. The figure also indicates that very good resolution can be obtained in principle for purely organic mixes at a few atmospheres pressure. These gas choices, which might be practical for small vertex detection chambers, typically require rather high voltages (up to a factor of two compared to Argon rich mixes at atmospheric pressure) to get to a reasonable gas gain.

For a configuration where E and B are parallel (TPC configuration) the diffusion can be substantially

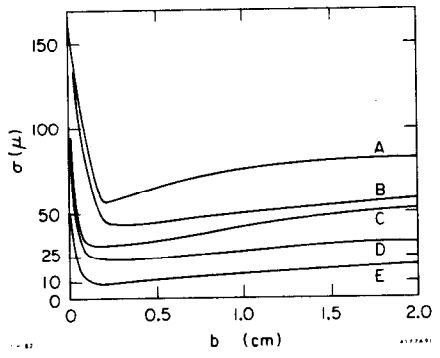

Fig. 1. Model calculations for resolution versus track impact parameter. Curves are:
A - 50/50 Argon/Ethane at 1 atm.
B - Pure Ethane at 1 atm.
C - 50/50 Argon/Ethane at 2 atm.
D - Pure Ethane at 2 atm.
E - Pure Isobutane at 3 atm.

reduced because of the magnetic field.[5]

Dual-Track Separability for a Parallel Wire Grid

The use of a multi-sense-wire cell allows one to control the ionization sampling and thus the double track separation that is possible in the cell. Figure 2

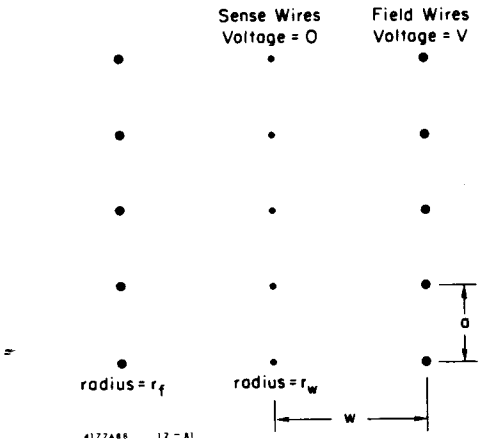

Fig. 2. Multi-sense-wire cell using parallel wire grids.

shows a section of a simple multi-wire cell which is taken as rectangular in shape for simplicity. We look at this simplest parallel wire array since it illustrates the essentials of the problem. The main parameters describing the cell are:

r_w = radius of a sense wire.

r_f = radius of a field wire.

E_w = electric field at the surface of a sense wire.

E_{cell} = nearly constant drift field over the bulk of the cell.

a = spacing between wires along the sense wire plane (radial direction).

w = cell half-width.

The cell height has to be $\geq$ 1.5 w to get reasonably uniform behavior for all the inner sense wires. In the following discussion all field wires and sense wires are assumed to be at a potential V and at ground respectively. To reduce cross-talk, every second wire in the sense plane can be taken to be thicker so it does not amplify and thus is not read-out. In this case the spacing between the sense wires used is actually = 2a. We do not discuss here in detail the case of negative voltage on these thicker wires, which can be used to reduce V, and which can be explored as an interesting added degree of freedom.[8] The case of no negative voltage gives the best dual-track resolution for a given spacing a.

This type of cell is sufficiently simple that its behavior can be thought of as follows: (for simplicity in the discussion we chose the same radius r_w for all sense plane wires)

1. Near each wire we have a roughly radial field varying as 1/r. This near region extends to a radius $\simeq a/\pi$.
2. The rest of the cell has a nearly constant drift field E_{cell}. Using Gauss' law the field on the sense wires and E_{cell} are related by:

$$E_{cell} = \left[\frac{\pi r_w}{a}\right] E_w$$

Note: E_w is fixed by the chamber gain for a given r_w. $r_w E_w$ is ~ 250-350 volts for typical wires, gains and gases. Thus for a = 1 cm we expect E_{cell} = 1 kV/cm which is a typical value.

3. The cell dimension w enters only into the determination of the absolute voltage, V, on the field wires. Integrating from a sense to a field wire using a 1/r field within a/π of a wire and E_{cell} elsewhere gives a good estimate:

$$V = E_{cell}\left[(w - \frac{2a}{\pi}) + \frac{a}{\pi}\,\ell n\,(\frac{a}{\pi r_w}) + \frac{a}{\pi}\,\ell n\,(\frac{a}{\pi r_f})\right].$$

4. The trajectories of typical drifting ionization electrons are shown in Figure 3 for the case of no magnetic field. For the inner wires in the cell the trajectories are parallel straight lines till they reach the near region. Looking at the figure the maximum path difference among the ionization electrons produced by one normally incident

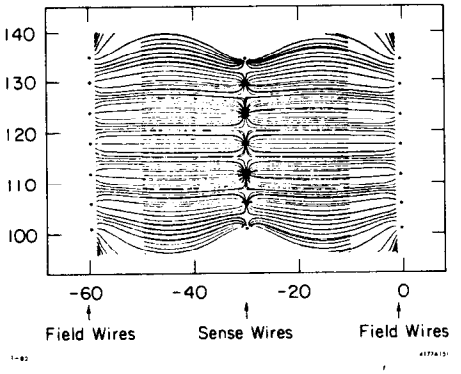

Fig. 3. Representative electron drift trajectories for several normally incident tracks. Cell half-width = 3 cm, wire separation = 6 mm. For simplicity B has been taken = 0.

particle is = a/2. If we want the arrival of all ionization electrons from two normally incident particles to be separated in time, then the two particles must be incident at impact parameters separated by > a/2. Thus a/2 is approximately the dual-track separation distance for the cell. Note, the result depends on the extent of the 1/r near region, which provides the dual-track limit for other parallel wire arrays.

5. For incidence at an angle θ to the normal, the maximum path difference is $\simeq \frac{a}{2}(1+\tan\theta)$. The dual-track resolution is not seriously degraded by non-normal incidence, provided $\tan\theta \lesssim 1/2$, which occurs at 26° which is a large bend angle. Note, the Lorentz-Angle acts as an additional angle adding or subtracting from θ depending on the track orientation and thus should be minimized.

To check the above characteristics quantitatively, we have looked at the drift cell of Figure 3 for the case a = 6 mm and w = 3 cm.[9] For this case E_{cell} = 1.5 kV/cm. The large value of E_{cell} helps decrease the Lorentz-Angle. Using a Monte Carlo program which generates and follows ionization electrons produced in the cell, Figure 4 shows the distribution of collected

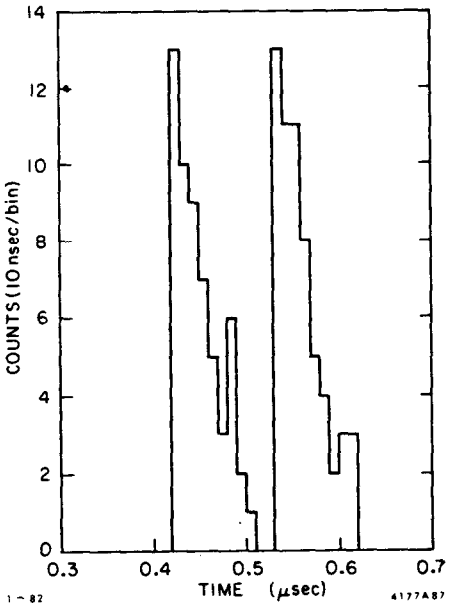

Fig. 4. Ionization electron arrival time spectra produced by two normally incident tracks whose impact parameters are separated by 3 mm in space. Cell is that shown in Fig. 3, but now with B = 5 kG.

electrons from two normally incident tracks whose impact parameters differ by 3 mm. The calculation has been done with a 5 kG field and 90/10 Ar/CH_4 gas. The variation of the drift velocity with the local electric field, as well as the local Lorentz-Angle, has been included in the calculation. A dual-track separation of 3 mm should be attainable for such a cell using electronics which suppresses the 1/t pulse tail.

We might ask what the limit on dual-track separability is for a parallel array if we use standard leading edge discrimination only. Since wire separations of about 1 to 2 mm are at the limit of what's possible we can expect a limit ~ 1 mm if we stick to standard techniques.

Quality of Information for Pattern Recognition

Drift chamber information is typically used at two stages, the first is for pattern recognition where one would like to get good initial estimates of positions and angles for sorting the left-right ambiguity and linking points or track elements, the second is for high precision fitting of track parameters.

In general, pattern recognition problems will occur for the few tracks which are close together in an event. For a system of single-hit small cells the randomization of the wire pattern from layer to layer tends to provide hits on some layers for each of two tracks which are spatially close together. Thus if the pattern recognition program can find tracks with some missing hits it can handle most of the close tracks.

For a multi-sense-wire cell, with multi-hit electronics, track separations at the few mm level are possible as seen in the previous section. In addition the nearly uniform electric field allows very good precision for certain quantities prior to angular corrections. As an example we can look at the solution of the left-right ambiguity by wire staggering.

If alternate sense wires are staggered by ±δ we can resolve the left-right ambiguity in an individual cell before pattern recognition. Taking the example of staggered wire triplets, the quantity

$$\Delta = v_{Drift}\left[\frac{t_1 + t_3}{2} - t_2\right]$$

where the t_i are the measured times, is centered at ± 2δ with the sign giving the side of the cell traversed. Thus if 4δ >> error on Δ we can resolve the left-right ambiguity. Using $\sigma_\Delta = \sqrt{\frac{3}{2}}\,\sigma_x$, with σ_x = 200 μm, gives δ ≃ 280 μm if we want $4\delta = 5\sigma_\Delta$. Figure 5 shows a plot

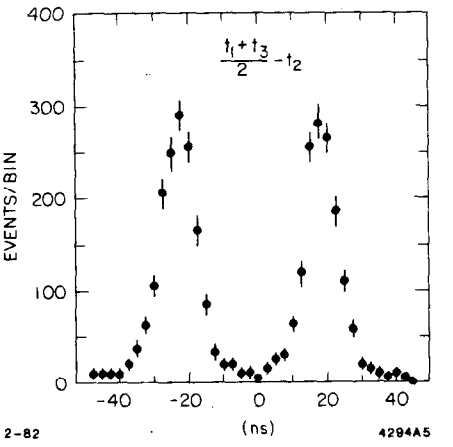

Fig. 5. Correlation of drift times $\frac{t_1 + t_3}{2} - t_2$ into two peaks for a cell with three staggered sense wires. Data is from the MARK III Drift Chamber.

of Δ for data from the MARK III chamber, for which δ ≃ 400 μm. The constraint on the three times provided by Δ allows the use of the very good resolution of the chamber for the rejection of spurious hits (multi-pulsing, single bremsstrahlung conversions, poorly measured points due to δ-rays, confused points due to crossing tracks in the cell) before pattern recognition begins. This could be particularly useful in an environment containing many soft photons or neutrons which might give a fair number of single hits but very few valid triplets.

To understand why Δ can be measured so accurately we will look at the space-time relation for a parallel

wire array. For concreteness we take the cell used as an example in the previous section. The drift consists of:

1. Uniform drift along the direction given by the Lorentz-Angle for ionization produced in the far region where $E = E_{cell}$.
2. Drift along radius in near region, for radius $\leq a/\pi$. The velocity here can be different than in the uniform region, depending on the gas. We assume below that only one velocity describes the drift in both regions.

The earliest arriving electron trajectories for a track are shown in Figure 6. Measuring distances along the direction for the uniform part of the drift and taking $v_{Drift}t$ as the estimate of the distance:

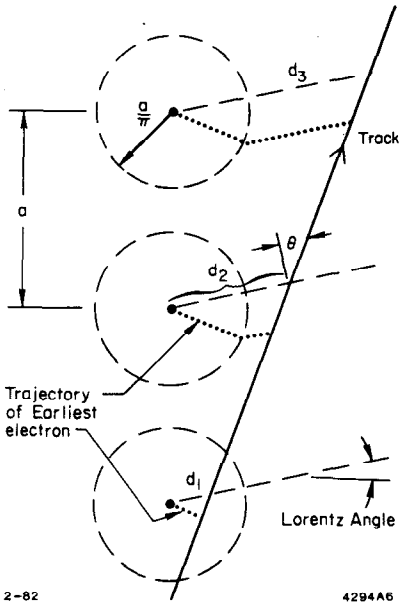

Fig. 6. Relation of drift distance measured and the distance along a line given by the Lorentz-Angle. In the near region:

$$d_1 = v_{Drift}t_1/\cos\theta.$$

In the far region:

$$d_2 = v_{Drift}t_2 + \frac{a}{\pi}\left(\frac{1}{\cos\theta} - 1\right)$$

$$d_3 = v_{Drift}t_3 + \frac{a}{\pi}\left(\frac{1}{\cos\theta} - 1\right)$$

1. Corrections to the estimated distance in the near region go like $1/\cos(\theta)$. For normal incidence this is $1/\cos(\theta_L)$.
2. The correction over most of the cell is proportional to a/π and thus is expected to be small for the case $a \simeq 6$ mm discussed in the previous section.
3. Since the angular correction is a constant for hits not too close to the wire, several quantities for which the correction cancels can be calculated very accurately, for example:
   a) $\frac{d_1 + d_2}{2} - d_2$, used to solve the left-right ambiguity.
   b) $d_3 - d_1$, which gives a numerical evaluation of $\frac{d\rho}{d\phi}$, the local tangent to the track. These can be taken at the track finding level to be accurate to a few hundred microns.

REFERENCES

1. Segmentation requirements have been studied both in the SLAC Linear Collider workshop and several LEP workshops. See, for example, K. Winter, "Experimentation at LEP; Hadronic Final States", 1979 LEP Study, p. 93.
2. Examples of chambers with small cells are those used in the: MARK II, CLEO, and ARGUS detectors. A discussion of the use of such chambers at higher energies can be found in:
   K. Berkelman, Cornell Z^0 Workshop, CLNS 81-490, p. 58.
   G. Trilling, SLAC Linear Collider Note #46.
3. Examples of such chamber are those used in the JADE, AFS and MARK III detectors. A description of most of the presently operating chambers can be found in:
   Physica Scripta Vol. 23, 1981.
4. R.A. Boie, et al., IEEE Trans on Nucl. Sci., NS-28, 603 (1981).
5. For details on the TPC see PEP Proposal #4, 1976.
6. For a recent look at some gases, as well as references to earlier work, see:
   G. Baranko, SLAC Linear Collider Note #45.
7. J. Jaros, SLAC Linear Collider Note #51.
8. J. Va'Vra and L. Roberts, SLAC Linear Collider Note #31.
9. F. Grancagnolo, A. Seiden, D.B. Smith, SLAC Linear Collider Note #36.